



## Three years of Ulysses dust data: 2005 to 2007

H. Krüger<sup>a,b,\*</sup>, V. Dikarev<sup>c</sup>, B. Anweiler<sup>b</sup>, S.F. Dermott<sup>d</sup>, A.L. Graps<sup>e</sup>, E. Grün<sup>b,f</sup>, B.A. Gustafson<sup>d</sup>, D.P. Hamilton<sup>g</sup>, M.S. Hanner<sup>h</sup>, M. Horányi<sup>f</sup>, J. Kissel<sup>a</sup>, D. Linkert<sup>b</sup>, G. Linkert<sup>b</sup>, I. Mann<sup>i</sup>, J.A.M. McDonnell<sup>j</sup>, G.E. Morfill<sup>k</sup>, C. Polanskey<sup>l</sup>, G. Schwehm<sup>m</sup>, R. Srama<sup>b,n</sup>

<sup>a</sup> Max-Planck-Institut für Sonnensystemforschung, 37191 Katlenburg-Lindau, Germany

<sup>b</sup> Max-Planck-Institut für Kernphysik, 69029 Heidelberg, Germany

<sup>c</sup> Fakultät für Physik, Universität Bielefeld, Postfach 100131, 33501 Bielefeld, Germany

<sup>d</sup> University of Florida, 211 SSRB, Campus, Gainesville, FL 32609, USA

<sup>e</sup> Department of Space Studies, Southwest Research Institute, 1050 Walnut Street Suite 300, Boulder, CO 80302, USA

<sup>f</sup> Laboratory for Atmospheric and Space Physics, University of Colorado, Boulder, CO 80309, USA

<sup>g</sup> University of Maryland, College Park, MD 20742-2421, USA

<sup>h</sup> Astronomy Department, 619 LGRT, University of Massachusetts, Amherst, MA 01003, USA

<sup>i</sup> School of Science and Engineering, Kindai University, Kowakae 3-4-1, Higashi-Osaka, Osaka 577-8502, Japan

<sup>j</sup> Planetary and Space Science Research Institute, The Open University, Milton Keynes MK7 6AA, UK

<sup>k</sup> Max-Planck-Institut für Extraterrestrische Physik, 85748 Garching, Germany

<sup>l</sup> Jet Propulsion Laboratory, Pasadena, CA 91109, USA

<sup>m</sup> ESAC, PO Box 78, 28691 Villanueva de la Cañada, Spain

<sup>n</sup> Universität Stuttgart, Institut für Raumfahrtssysteme, Pfaffenwaldring 31, 70569 Stuttgart, Germany

### ARTICLE INFO

#### Article history:

Received 6 August 2009

Received in revised form

2 November 2009

Accepted 3 November 2009

Available online 12 November 2009

#### Keywords:

Interstellar dust

Interplanetary dust

Dust dynamics

Interstellar medium

Dust in-situ measurements

### ABSTRACT

The Ulysses spacecraft has been orbiting the Sun on a highly inclined ellipse ( $i = 79^\circ$ , perihelion distance 1.3 AU, aphelion distance 5.4 AU) since it encountered Jupiter in February 1992. Since then it has made almost three revolutions about the Sun. Here we report on the final three years of data taken by the on-board dust detector. During this time, the dust detector recorded 609 dust impacts of particles with masses  $10^{-16} \text{ g} \leq m \leq 10^{-7} \text{ g}$ , bringing the mission total to 6719 dust data sets. The impact rate varied from a low value of 0.3 per day at high ecliptic latitudes to 1.5 per day in the inner solar system. The impact direction of the majority of impacts between 2005 and 2007 is compatible with particles of interstellar origin; the rest are most likely interplanetary particles. We compare the interstellar dust measurements from 2005/2006 with the data obtained during earlier periods (1993/1994) and (1999/2000) when Ulysses was traversing the same spatial region at southern ecliptic latitudes but the solar cycle was at a different phase. During these three intervals the impact rate of interstellar grains varied by more than a factor of two. Furthermore, in the two earlier periods the grain impact direction was in agreement with the flow direction of the interstellar helium while in 2005/2006 we observed a shift in the approach direction of the grains by approximately  $30^\circ$  away from the ecliptic plane. The reason for this shift remains unclear but may be connected with the configuration of the interplanetary magnetic field during solar maximum. We also find that the dust measurements are in agreement with the interplanetary flux model of Staubach et al. (1997) which was developed to fit a 5-year span of Ulysses data.

© 2009 Elsevier Ltd. All rights reserved.

## 1. Introduction

Ulysses has been the only space mission so far that left the ecliptic plane and passed over the poles of the Sun. The spacecraft was launched in 1990 and was very successfully operated until 30 June 2009, although individual instruments had to be turned off

to conserve power. Its orbital plane was almost perpendicular to the ecliptic plane ( $79^\circ$  inclination) with an aphelion at Jupiter. This special orbit orientation allowed Ulysses to unambiguously detect interstellar dust grains entering the heliosphere because the spacecraft's orbital plane was almost perpendicular to the flow direction of the interstellar dust. Ulysses had a highly sensitive impact ionisation dust detector on board which measured impacts of micrometre and sub-micrometre dust grains. The detector was practically identical with the dust

E-mail address: [krueger@mps.mpg.de](mailto:krueger@mps.mpg.de) (H. Krüger).

instrument which flew on board the Galileo spacecraft. Both instruments were described in previous publications by Grün et al. (1992a, b, 1995c).

### 1.1. Summary of results from the Ulysses dust investigations

Comprehensive reviews of the scientific achievements of the Ulysses mission including results from the dust investigation were given by Balogh et al. (2001) and Grün et al. (2001). References to other works related to Ulysses and Galileo measurements on dust in the planetary system were also given by Grün et al. (1995a, b); Krüger et al. (1999a, b, 2001a, b, 2006b, a); Krüger and Grün (2009). Some mission highlights are also summarised in Table 1.

Various dust populations were investigated with the Ulysses and Galileo dust experiments in interplanetary space: the interplanetary dust complex including  $\beta$ -meteoroids (i.e. dust particles which leave the solar system on unbound orbits due to acceleration by radiation pressure), interstellar grains sweeping through the heliosphere, and dust stream particles expelled from the Jovian system by electromagnetic forces, to name only the most significant dust types detected with Ulysses which have been analysed so far. In the following, we summarise the most significant achievements of the Ulysses dust measurements.

Ulysses and Galileo dust measurements were used to study the 3-dimensional structure of the interplanetary dust complex and its relation to the underlying populations of parent bodies like asteroids and comets (Divine, 1993; Grün et al., 1997; Staubach et al., 1997). Studies of asteroidal dust released from the IRAS dust bands show that they are not efficient enough dust sources to maintain the observed interplanetary dust cloud (Mann et al., 1996). The state of the inner solar system dust cloud within approximately 1 AU from the Sun including dust destruction and ion formation processes in relation to so-called solar wind pickup ions detected by the Solar Wind Ion Composition Spectrometer (SWICS) onboard Ulysses was investigated (Mann et al., 2004; Mann and Czechowski, 2005). An improved physical model was developed for the interplanetary meteoroid environment (Dikarev et al., 2002, 2005) which uses long-term particle dynamics to define individual interplanetary dust populations. The Ulysses and Galileo in situ dust data are an important data set for the validation of this model. The properties of  $\beta$ -meteoroids were also studied with the Ulysses data set (Wehry and Mann, 1999; Wehry et al., 2004). Finally, the potential connection of cometary dust trails and enhancements of the interplanetary magnetic field as measured by Ulysses was discussed by Jones and Balogh (2003).

During its first flyby at Jupiter in 1992, the Ulysses dust instrument discovered burst-like intermittent streams of

approximately 10 nm sized dust grains in interplanetary space (Grün et al., 1993) which had been emitted from the Jovian system (Hamilton and Burns, 1993; Horányi et al., 1993; Zook et al., 1996). This discovery was completely unexpected as no periodic phenomenon for tiny dust grains in interplanetary space was previously known. These grains strongly interacted with the interplanetary and the Jovian magnetic fields (Horányi et al., 1997; Grün et al., 1998) and the majority of them originated from Jupiter's moon Io (Graps et al., 2000). In February 2004 Ulysses had its second Jupiter flyby (at 0.8 AU distance from the planet) and again measured the Jovian dust streams (Krüger et al., 2006c; Flandes and Krüger, 2007).

Another important discovery made with Ulysses were interstellar dust particles sweeping through the heliosphere (Grün et al., 1993). The grains which originated from the very local interstellar environment of our solar system were identified by their impact direction and impact speed, the latter being compatible with particles moving on hyperbolic heliocentric trajectories (Grün et al., 1994). Their dynamics depends on the grain size and is strongly affected by the interaction with the interplanetary magnetic field and by solar radiation pressure (Landgraf et al., 1999; Landgraf, 2000; Mann and Kimura, 2000; Czechowski and Mann, 2003b, 2003a; Landgraf et al., 2003). As a result, the size distribution and fluxes of grains measured inside the heliosphere are strongly modified. Studies of the dust impacts detected with both Ulysses and Galileo showed that the intrinsic size distribution of interstellar grains in the local interstellar environment of our solar system extends to grain sizes larger than those detectable by spectroscopic observations of long sight-lines to stars, enabling information of intervening dust characteristics to be obtained (Frisch et al., 1999; Frisch and Slavin, 2003; Landgraf et al., 2000; Grün and Landgraf, 2000). Observations of radar meteors entering the Earth's atmosphere at high speeds also indicate the existence of even larger interstellar grains (Taylor et al., 1996; Baggaley and Neslušan, 2002).

The Ulysses and Galileo interstellar dust measurements showed that the dust-to-gas mass ratio in the local interstellar cloud is higher than the standard interstellar value derived from cosmic abundances (Landgraf, 1998; Frisch et al., 1999). This implied the existence of inhomogeneities in the diffuse interstellar medium on relatively small length scales. In 2005/2006 the Ulysses measurements showed a 30° shift in the impact direction of interstellar grains with respect to the interstellar helium flow (Krüger et al., 2007). The reason for this shift is presently unclear.

Finally, it turned out that the dust sensor side walls have a similar sensitivity to dust impacts as the detector target itself (Altobelli et al., 2004; Willis et al., 2005). This shows that earlier

**Table 1**  
Summary of Ulysses data papers, significant mission events and dust detector switch-off times.

Time interval	Significant mission events	Dust detector off	Paper number
1990–1992	Ulysses launch (6 October 1990), Jupiter flyby (8 February 1992, distance 6.3 R <sub>J</sub> )	Before 27 October 1990, 14 June 1991–18 June 1991	III (Grün et al., 1995a)
1993–1995	Maximum southern latitude -79° (3 October 1994), Perihelion (12 March 1995), Maximum northern latitude 79° (19 August 1995)	8 August 1993–11 August 1993, 27 November 1993–28 November 1993, 10 October 1994–11 October 1994, 10 December 1995	V (Krüger et al., 1999b)
1996–1999	Aphelion (20 April 1998)	17 August 1996–18 August 1996, 1 April 1997–2 April 1997, 15 February 1999–16 February 1999	VII (Krüger et al., 2001b)
2000–2004	Maximum southern latitude -80° (27 November 2000), Perihelion (23 May 2001), maximum northern latitude 80° (13 October 2001), Jupiter flyby (4 February 2004, distance 0.8 AU), Aphelion (30 June 2004)	26 March 2002–8 April 2002, 1 December 2002–3 June 2003, 28 June 2003–22 August 2003, 30 November 2003–2 December 2003	IX (Krüger et al., 2006a)
2005–2007	Maximum southern latitude -80° (7 February 2007), Perihelion (18 August 2007)	28 September 2006—9 March 2007, 2 April 2007—30 April 2007, After 30 November 2007	XI (this paper)

investigations which neglected the contributions of the side wall overestimated the interstellar dust flux by about 20%. Since the contribution of the sensor side wall increases the effective dust instrument field-of-view, the velocity dispersion of the observed interstellar dust stream turned out to be smaller by about 30% than previously thought.

Due to its unique highly inclined heliocentric trajectory Ulysses was able to monitor interstellar dust at high ecliptic latitudes between 3 and 5 AU. Dust measurements between 0.3 and 3 AU in the ecliptic plane exist also from Helios, Galileo and Cassini. These data show evidence for distance-dependent alteration of the interstellar dust stream caused by radiation pressure, gravitational focussing and electromagnetic interaction of the grains with the time-varying interplanetary magnetic field (Altabelli et al., 2003, 2005a, b).

## 1.2. The Ulysses and Galileo dust data papers

The Ulysses dust detector obtained dust data for more than 17 years, making it the longest continually operating spaceborne dust detector to date. With the publication of this paper, the full Ulysses data set, along with 13 years of Galileo data, will be fully described in the scientific literature. The reduction process of Ulysses and Galileo dust data was described by Grün et al. (1995c, hereafter Paper I). In the odd-numbered Papers III, V, VII and IX (Grün et al., 1995a; Krüger et al., 1999b, 2001b, 2006a) we presented the Ulysses data set spanning the time period from launch in October 1990 to December 2004. The companion even-numbered Papers II, IV, VI and VIII (Grün et al., 1995b; Krüger et al., 1999a, 2001a, 2006b) discussed the 10 years of Galileo data from October 1989 to December 1999. The current paper (Paper XI) extends the Ulysses data set from January 2005 until the Ulysses dust measurements ceased in November 2007, and a companion paper (Krüger et al., 2010, Paper X) presents Galileo's final measurements at Jupiter from 2000 to 2003. A summary of the temporal and spatial coverage of our Ulysses data papers is given in Table 1.

The main data products are a table of the impact rate of all impacts determined from the particle accumulators and a table of both raw and reduced data of all dust impacts for which the full data set of measured impact parameters was transmitted to Earth. The information presented in these papers is similar to data which we have submitted to the various data archiving centres (Planetary Data System, NSSDC, Ulysses Data Centre). Electronic access to the data is also possible via the world wide web: <http://www.mpi-hd.mpg.de/dustgroup/>.

This paper is organised like our earlier Papers III, V, VII and IX. We begin with an overview of important events of the Ulysses mission between 2005 and 2007 (Section 2). Sections 3 and 4 describe and analyse the Ulysses dust data set for this period. In Section 5 we discuss the dust data set from the entire Ulysses mission, we analyse in particular the interstellar dust measurements obtained in the 2005–2007 interval, and we compare these results to previous ones. In Section 6 we summarise our conclusions.

## 2. Mission and instrument operation

### 2.1. Ulysses mission and dust instrument characteristics

The Ulysses spacecraft was launched on 6 October 1990. A swing-by manoeuvre at Jupiter in February 1992 rotated the orbital plane  $79^\circ$  relative to the ecliptic plane. On the resulting trajectory (Fig. 1) Ulysses finished two full revolutions about the Sun. Passages over the south pole of the Sun occurred in October

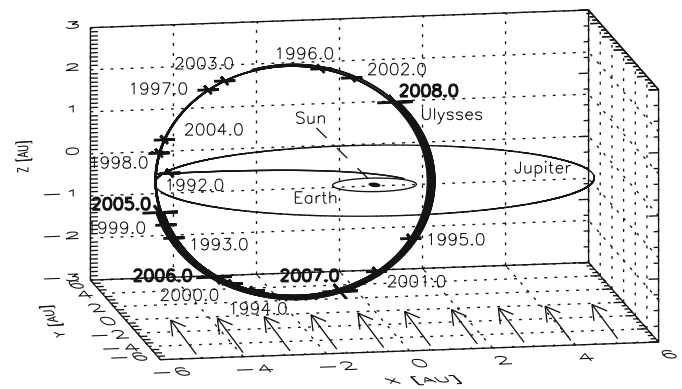


**Fig. 1.** The trajectory of Ulysses in ecliptic coordinates with the Sun at the centre. The orbits of Earth and Jupiter indicate the ecliptic plane, and the initial trajectory of Ulysses was in this plane. Since Jupiter flyby in early 1992 the orbit has been almost perpendicular to the ecliptic plane ( $79^\circ$  inclination). Crosses mark the spacecraft position at the beginning of each year. The 2005–2007 part of the trajectory is shown as a thick line. Vernal equinox is to the right (positive x axis). Arrows indicate the undisturbed interstellar dust flow direction which is within the measurement accuracy co-aligned with the direction of the interstellar helium gas flow. It is almost perpendicular to the orbital plane of Ulysses.

1994, November 2000 and February 2007, passages through the ecliptic plane at a perihelion distance of 1.3 AU occurred in March 1995, May 2001 and August 2007, and passes over the Sun's north pole were in August 1995, October 2001 and January 2008. In April 1998 and July 2004 the spacecraft crossed the ecliptic plane at an aphelion distance of 5.4 AU. Orbital elements for the out-of-ecliptic part of the Ulysses trajectory are given in Paper VII. Fig. 1 shows that during most of the time interval considered in this paper Ulysses was at southern ecliptic latitudes.

Ulysses is a spinning spacecraft, and the dust sensor orientation at the time of a dust particle impact is recorded, allowing for an independent determination of the grain impact direction. Ulysses spins at five revolutions per minute about the centre line of its high gain antenna which normally points at Earth. Fig. 2 shows the deviation of the spin axis from the Earth direction for the period 2005–2007. Most of the time the spin axis pointing was within  $1^\circ$  of the nominal Earth direction, similar to the mission before 2005. This small deviation is usually negligible for the analysis of measurements with the dust detector. The Ulysses spacecraft and mission are explained in more detail by Wenzel et al. (1992). Details about the data transmission to Earth can also be found in Paper III.

The Ulysses dust detector (GRU) has a  $140^\circ$  wide field of view and is mounted on the spacecraft nearly at right angles ( $85^\circ$ ) to the antenna axis (spacecraft spin axis). Due to this mounting geometry, the dust sensor is most sensitive to particles approaching from the plane perpendicular to the spacecraft–Earth direction. The impact direction of dust particles is measured by the rotation angle which is the sensor viewing direction at the time of a dust impact. During one spin revolution of the spacecraft the rotation angle scans through a complete circle of  $360^\circ$ . Zero degrees rotation angle is defined to be the direction closest to ecliptic north. At high ecliptic latitudes, however, the sensor pointing at  $0^\circ$  rotation angle significantly deviates from the actual north direction. During the passages over the Sun's polar regions the sensor always scans through a plane tilted by about  $30^\circ$  from the ecliptic plane and all rotation angles lie close to the ecliptic plane (cf. Fig. 4 in Grün et al., 1997). A sketch of the viewing geometry around aphelion passage can be found in Grün et al. (1993).

The available electrical power on board Ulysses became an issue beginning in 2001 due to decreasing power generation of the radioisotope batteries (RTGs). Some instrument heaters on

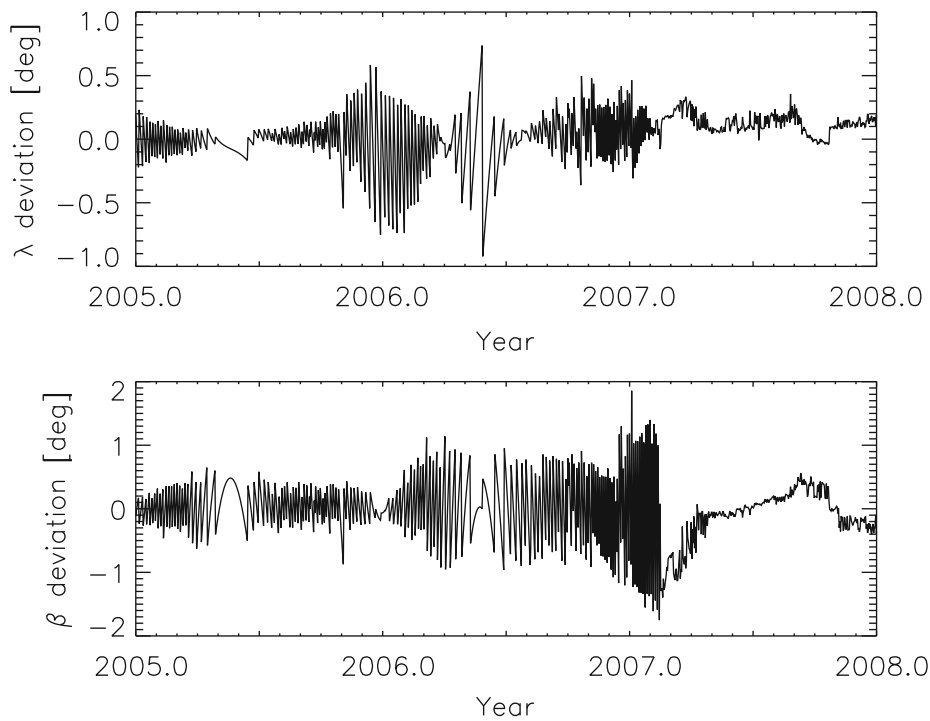


**Fig. 2.** Spacecraft attitude: deviation of the antenna pointing direction (i.e. positive spin axis) from the nominal Earth direction. The angles are given in ecliptic longitude (top) and latitude (bottom, equinox 1950.0).

board had to be switched off to save power which in turn also reduced the on board temperature. Later, in 2002, power consumption could not be sufficiently reduced anymore by simply switching off heaters, and a cycling instrument operation scheme had to be implemented: one or more of the scientific instruments had to be switched off at a time. In the 2005–2007 interval considered in this paper the dust instrument was switched off during a total time period of about seven months, separated into three individual time periods (see Section 2.2). After 30 November 2007 the dust instrument remained switched off permanently. It was planned to switch the dust instrument on in January 2008 again, but due to a failure on board the spacecraft, this did not happen. Hence, no dust data were obtained after 30 November 2007 although operation of the Ulysses spacecraft continued until 30 June 2009.

## 2.2. Dust instrument operation

Table 2 gives significant mission and dust instrument events from 2005 to 2007. Earlier events are only listed if especially significant. A comprehensive list of events from launch until the end of 2004 was given in Papers III, V, VII and IX.

During the earlier Ulysses mission phases until 2000, several spacecraft anomalies occurred during which all scientific instruments on board were switched off automatically (Disconnection of all Non-Essential Loads—DNELs for short). No such anomaly occurred in the 2005–2007 interval. The dust instrument was switched off between 28 September 2006 and 9 March 2007, from 2 April 2007 to 30 April 2007 and after 30 November 2007 (cf. Table 1), respectively, because there was no longer enough electrical power generated by the RTGs to further operate all instruments simultaneously.

The dust instrument has two heaters to allow for a relatively stable operating temperature within the sensor. By heating one of the two or both heaters, three different heating power levels can

be achieved (0.4, 0.8 or 1.2 W; for comparison, the total power consumption of the instrument without heaters is 2.2 W). Sensor heating was necessary when the spacecraft was outside about 2 AU because relatively little radiation was received from the Sun.

Before 2001 one or both heaters were switched on beyond 2 AU. Since November 2001 the maximum allowed heating power for nominal dust instrument operation has been limited to 0.8 W to save power on board Ulysses. This reduced the sensor temperature by about 10 °C as compared to the configuration with 1.2 W heating power at similar heliocentric distance. The full heating power was only allowed for short periods before instrument switch-on to avoid damage of the electronics. In 2005 and 2006 the instrument was operated with 0.8 W heating power, and in 2007 the heating power was set to 0.4 W, except during switch-ons when it was raised to 1.2 W.

Table 2 lists the total powers consumed by the heaters. From 2005 to 2007 the temperature of the dust sensor was between –37 and +16 °C. The lower limit for the specified operational range is –30 °C. No major effect of the reduced temperature was recognised (except for an anomalous temperature-related flipping in the housekeeping value of the channeltron high voltage in 2004, see Paper IX).

No reprogramming of the Ulysses dust instrument occurred in the 2005–2007 interval. In the earlier mission the instrument was reprogrammed three times and the reader is referred to Papers V and IX for details. In particular, a new classification scheme for impact events was implemented in April 2002 which is the same as the one installed in the Galileo instrument in July 1994 (Paper IV).

## 2.3. Instrument sensitivity and noise

Analysis of the in-orbit noise characteristics of the dust instrument (Paper III) led to a relatively noise-free configuration with which the instrument was normally operated until August 2000: channeltron voltage 1140 V (HV = 3); event definition status such that either the channeltron or the ion-collector



**Table 2**

Ulysses mission and dust detector (GRU) configuration, tests and other events.

Yr—day	Date	Time	Event
1990—279	06.10.90		Ulysses launch
2003—154	03.06.03	03:38	GRU 0.8 W heater on
2004—182	30.06.04		Ulysses aphelion passage (5.4 AU)
2004—337	02.12.04	11:00	GRU nominal configuration: HV = 4, EVD = C,I, SSEN = 0001
2005—006	06.01.05	07:00	GRU noise test
2005—034	03.02.05	04:20	GRU noise test
2005—063	04.03.05	03:00	GRU noise test
2005—090	31.03.05	01:00	GRU noise test
2005—120	30.04.05	00:00	GRU noise test
2005—146	26.05.05	04:00	GRU noise test
2005—174	23.06.05	20:00	GRU noise test
2005—201	20.07.05	17:27	GRU noise test
2005—229	17.08.05	11:49	GRU noise test
2005—259	16.09.05	19:00	GRU noise test
2005—285	12.10.05	09:00	GRU noise test
2005—314	10.11.05	13:14	GRU noise test
2005—342	08.12.05	11:00	GRU noise test
2006—005	05.01.06	08:30	GRU noise test
2006—033	02.02.06	09:16	GRU noise test
2006—061	02.03.06	04:00	GRU noise test
2006—089	30.03.06	02:00	GRU noise test
2006—118	28.04.06	00:30	GRU noise test
2006—148	28.05.06	06:28	GRU noise test
2006—173	22.06.06	07:33	GRU noise test
2006—202	21.07.06	19:00	GRU noise test
2006—232	20.08.06	17:00	GRU noise test
2006—256	13.09.06	20:11	GRU noise test
2006—271	28.09.06	16:28	GRU off (both heaters off)
2007—038	07.02.07		Ulysses maximum south solar latitude (-79.7°)
2007—067	08.03.07	18:08	GRU 0.8 W heater on
2007—067	08.03.07	18:28	GRU 0.4 W heater on
2007—068	09.03.07	16:44	GRU 0.8 W heater off
2007—068	09.03.07	17:31	GRU on
2007—069	10.03.07	07:54	GRU nominal configuration
2007—079	20.03.07	08:40	GRU noise test
2007—092	02.04.07	18:11	GRU off (both heaters off)
2007—120	30.04.07	01:23	GRU 0.8 W heater on
2007—120	30.04.07	01:33	GRU 0.4 W heater on
2007—120	30.04.07	21:37	GRU 0.8 W heater off
2007—120	30.04.07	21:38	GRU on
2007—121	01.05.07	04:07	GRU nominal configuration
2007—130	10.05.07	20:00	GRU noise test
2007—158	07.06.07	01:00	GRU noise test
2007—187	06.07.07	16:15	GRU noise test
2007—214	02.08.07	01:53	GRU noisetest
2007—231	18.08.07		Ulysses perihelion passage (1.39 AU)
2007—232	19.08.07		Ulysses ecliptic plane crossing
2007—242	30.08.07	00:17	GRU noise test
2007—270	27.09.07	17:00	GRU noise test
2007—298	25.10.07	13:00	GRU noise test
2007—326	22.11.07	15:00	GRU noise test
2007—334	30.11.07	16:20	GRU off (both heaters off)
2008—014	14.01.08		Ulysses maximum north solar latitude (79.8°)
2009—181	30.06.09		Ulysses end of mission

Only selected events are given before 2005. See Section 2 for details. Abbreviations used: HV: channeltron high voltage step; EVD: event definition; ion—(I), channeltron—(C), or electron-channel (E); SSEN: detection thresholds, ICP, CCP, ECP and PCP. Times when no data could be collected with the dust instrument: 28 September 2006 to 9 March 2007, 2 April to 30 April 2007 and after 30 November 2007.

channel could, independent of each other, start a measurement cycle (EVD = C, I); detection thresholds for ion-collector, channeltron and electron-channel set to the lowest levels and the detection threshold for the entrance grid set to the first digital step (SSEN = 0, 0, 0, 1). See Paper I for a description of these terms.

During the entire Ulysses mission dedicated noise tests were performed at monthly intervals in order to monitor instrument health and noise characteristics. During all these tests the operational settings were changed in four steps at 1-h intervals, starting from the nominal configuration described above: (a) set the event definition status such that the channeltron, the ion collector and the electron-channel can initiate a measurement cycle (EVD = C, I, E); (b) set the thresholds for all channels to their

lowest levels (SSEN = 0, 0, 0, 0); (c) reset the event definition status to its nominal configuration (EVD = C, I) and increase the channeltron high voltage by one step with respect to the nominal configuration; and (d) reset the instrument to its nominal configuration (i.e. reduce the channeltron high voltage by one step and set the detection thresholds to SSEN = 0, 0, 0, 1).

The noise tests performed in the earlier mission before 2000 revealed a long-term drop in the noise sensitivity of the instrument which was most likely caused by a reduction in the channeltron amplification due to electronics degradation (Paper IX and Krüger et al., 2005). To counterbalance the reduced amplification we increased the channeltron high voltage by one digital step in August 2000 (HV = 4, 1250 V) which raised the

instrument sensitivity close to its original value from the earlier mission again (Paper IX). Although the aging of the channeltron led to a drop in the number of class 3 impacts, the dust impacts which have caused these events should have shown up in lower quality classes (cf. Section 3 and Paper IV for a definition of the quality classes). The noise response of the Ulysses dust detector was monitored since then and no significant drop in the sensitivity was recognised. In the time interval considered here HV = 4, EVD = C, I, SSEN = 0001 was the nominal configuration of the dust instrument (during noise tests the channeltron voltage was always raised by one digital step, i.e. to HV = 5, 1370 V).

Fig. 3 shows the noise rate of the dust instrument for the 2005–2007 period. The upper panel shows the daily maxima of the noise rate. In the earlier mission before November 2001 the daily maxima were dominated by noise due to interference with the sounder of the Unified Radio and Plasma wave instrument (URAP) on board Ulysses (Stone et al., 1992). Since November 2001 the sounder was switched off permanently for power saving and no sounder noise occurred any more (see Papers III, V, VII and IX for details of the sounder operation and sounder-related noise). Individual sharp spikes in the upper panel of Fig. 3 are caused by noise tests which occurred at approximately monthly intervals. They are best seen in 2007 when Ulysses was close to the Sun which is known to be a strong source of noise.

The bottom panel of Fig. 3 shows the daily averages in the noise rate. The average was about 10 events per day at random times and it shows that dead time is negligible. These noise rates are very similar to those measured since August 2000 (Paper IX) when the instrument was operated with the same channeltron

voltage as in the 2005–2007 interval, implying that no significant channeltron degradation has occurred since 2000.

### 3. Impact events

The dust instrument classifies all impact events into four classes and six ion charge amplitude ranges which leads to 24 individual categories, with one accumulator belonging to one individual category. Class 3, our highest class, are real dust impacts and class 0 are mostly noise events. Depending upon the noise of the charge measurements, classes 1 and 2 can be true dust impacts or noise events. Two classification schemes were used in the Ulysses dust instrument: since 26 March 2002, when the dust instrument was reprogrammed, the classification scheme has been the same as the one used in the Galileo instrument (described in Paper IV). A different scheme was used before which is described in Paper I.

Between 1 January 2005 and 30 November 2007 the complete data sets (sensor orientation, charge amplitudes, charge rise times, etc.) of 6970 events including 609 dust impacts were transmitted to Earth. Table 3 lists the number of all dust impacts counted with the 24 accumulators of the instrument. ‘ACxy’ refers to class number (CLN) ‘x’ and amplitude range (AR) ‘y’ (for a detailed description of the accumulator categories see Paper I). As discussed in the previous section, most noise events were recorded during the time periods when the dust instrument was configured to its high sensitive state for noise tests. During these periods many events were only counted by one of the 24 accumulators because their full information was overwritten before the data could be transmitted to Earth. Since the dust impact rate was low during times outside these periods, it is expected that only the data sets of very few true dust impacts were lost.

Appendix Table A1 lists all 609 particles detected between January 2005 and November 2007 for which the complete information exists. Note that approximately 45 Jovian stream particles were detected in six dust streams in 2005 (AR1, Krüger et al., 2006c) which are about 10 nm in size and their speeds exceed  $200 \text{ km s}^{-1}$  (Zook et al., 1996). Their mass and speed calibration is unreliable because their masses and speeds are outside of the calibration range of the dust instrument. Instead, Zook et al. obtained the particle speeds from dynamical modelling of the dust interaction with the ambient interplanetary magnetic field.

In Appendix Table A1 dust particles are identified by their sequence number and their impact time. The event category—class (CLN) and amplitude range (AR)—are given. Raw data as transmitted to Earth are displayed in the next columns: sector value (SEC) which is the spacecraft spin orientation at the time of impact, impact charge numbers (IA, EA, CA) and rise times (IT, ET), time difference and coincidence of electron and ion signals (EIT, EIC), coincidence of ion and channeltron signal (IIC), charge reading at the entrance grid (PA) and time (PET) between this signal and the impact. Then the instrument configuration is given: event definition (EVD), charge sensing thresholds (ICP, ECP, CCP, PCP) and channeltron high voltage step (HV). See Paper I for further explanation of the instrument parameters.

The next four columns in Appendix Table A1 give information about Ulysses’ orbit: heliocentric distance ( $R$ ), ecliptic longitude and latitude (LON, LAT) and distance from Jupiter ( $D_{\text{Jup}}$ , in astronomical units). The next column gives the rotation angle (ROT) as described in Section 2. Then follows the pointing direction of the dust instrument at the time of particle impact in ecliptic longitude and latitude ( $S_{\text{LON}}$ ,  $S_{\text{LAT}}$ ). Mean impact velocity ( $v$ , in  $\text{km s}^{-1}$ ) and velocity error factor (VEF, i.e. multiply or divide stated velocity by VEF to obtain upper or lower limits) as well as mean particle mass ( $m$ , in grams) and mass error factor (MEF) are

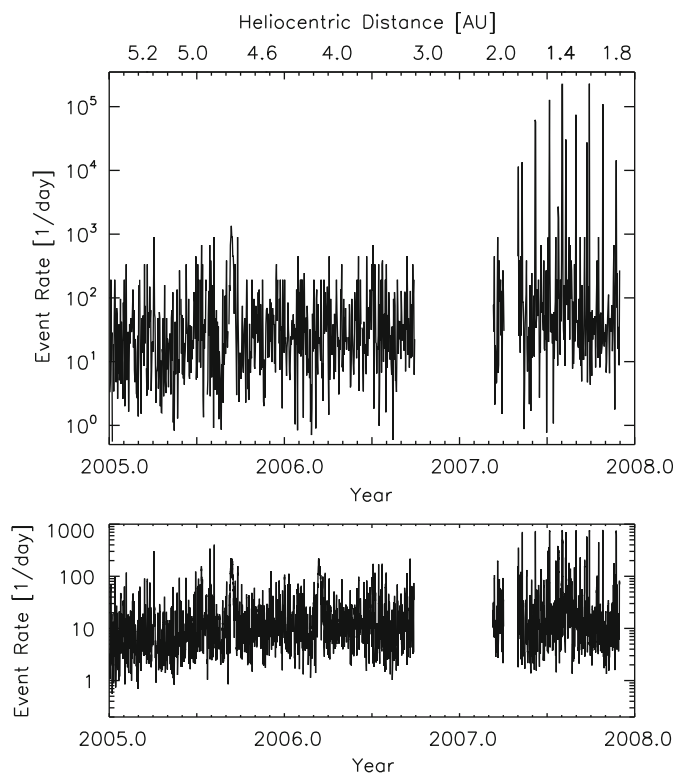


Fig. 3. Noise rate (class 0 events) detected with the dust instrument. The heliocentric distance of Ulysses is indicated at the top. Upper panel: Daily maxima in the noise rate (determined from the AC01 accumulator). Sharp spikes which are strongest after May 2008 when Ulysses was in the inner solar system are caused by periodic noise tests. Lower panel: One-day average of the noise rate calculated from the number of AC01 events for which the complete information was transmitted to Earth.

**Table 3**  
Overview of dust impacts detected with the Ulysses dust detector between 1 January 2005 and 30 November 2007 as derived from the accumulators.<sup>a</sup>

Date	Time	R [AU]	Δt [d]	AC 01 <sup>a</sup>	AC 11 <sup>a</sup>	AC 21	AC 31	AC 02 <sup>a</sup>	AC 12	AC 22	AC 32	AC 03	AC 13	AC 23	AC 33	AC 04	AC 14	AC 24	AC 34	AC 05	AC 15	AC 25	AC 35	AC 06	AC 16	AC 26	AC 36	
2005—006	11:45	5.300	7.561	–	–	–	–	–	–	–	1	–	–	–	–	–	–	–	1	*b	–	–	–	*b	–	–	–	
2005—039	23:36	5.258	33.49	–	1	11	2	–	–	5	2	–	–	–	–	–	–	–	–	*b	–	–	–	*b	–	–	–	
2005—061	19:36	5.227	21.83	–	3	8	3	–	–	–	2	–	–	–	1	–	–	–	1	*b	–	–	–	*b	–	–	–	
2005—089	09:46	5.184	27.59	–	1	11	3	–	1	5	2	–	–	–	1	–	–	–	–	*b	–	–	–	*b	–	–	–	
2005—104	17:01	5.158	15.30	–	–	4	2	–	–	3	–	–	–	–	–	–	–	–	1	*b	–	–	–	*b	–	–	–	
2005—140	22:27	5.089	36.22	–	5	6	1	–	–	5	2	–	–	–	–	–	–	–	1	*b	–	–	–	*b	–	–	–	
2005—177	01:56	5.013	36.14	–	5	4	2	–	–	9	9	–	–	–	–	–	–	–	–	*b	–	–	–	*b	–	–	–	
2005—204	13:40	4.949	27.48	–	2	5	1	–	–	2	2	–	–	–	3	–	–	–	–	*b	–	–	–	*b	–	–	–	
2005—227	18:13	4.891	23.18	–	4	5	2	–	–	3	7	–	–	–	1	6	–	–	–	*b	–	–	–	*b	–	–	–	
2005—250	17:23	4.831	22.96	–	1	6	–	–	1	1	7	–	–	–	2	–	–	–	1	*b	–	–	–	*b	–	–	–	
2005—284	14:06	4.734	33.86	–	2	3	–	–	–	2	4	–	–	1	7	–	–	–	–	*b	–	–	–	*b	–	–	–	
2005—310	21:37	4.654	26.31	–	1	3	–	–	–	5	5	–	–	–	3	–	–	–	–	*b	–	–	–	*b	–	–	–	
2005—337	10:38	4.568	26.54	–	3	–	–	–	–	2	2	–	–	–	1	–	–	–	1	*b	–	–	–	*b	–	–	–	
2005—364	06:07	4.475	26.81	–	1	–	–	–	–	1	1	–	–	–	1	–	–	–	–	*b	–	–	–	*b	–	–	–	
2006—028	18:17	4.368	29.50	–	2	2	1	–	1	3	4	–	–	–	1	–	–	–	–	*b	–	–	–	*b	–	–	–	
2006—052	22:35	4.274	24.17	–	2	3	–	–	–	2	4	–	–	–	2	–	–	–	–	*b	–	–	–	*b	–	–	–	
2006—078	05:59	4.172	25.30	–	2	2	–	–	–	1	–	–	–	–	3	–	–	–	–	*b	–	–	–	*b	–	–	–	
2006—100	06:53	4.078	22.03	–	–	1	–	–	–	3	1	–	–	–	1	1	–	–	–	*b	–	–	–	*b	–	–	–	
2006—132	07:12	3.935	32.01	–	–	2	–	–	–	2	1	–	–	–	5	–	–	–	–	*b	–	–	–	*b	–	–	–	
2006—165	22:45	3.776	33.64	–	1	2	1	–	–	1	2	–	–	–	2	–	–	–	1	*b	–	–	–	*b	–	–	–	
2006—192	21:07	3.642	26.93	–	–	1	–	–	–	1	1	–	–	–	1	–	–	–	–	*b	–	–	–	*b	–	–	–	
2006—217	08:19	3.514	24.46	–	1	1	–	–	–	–	1	–	–	–	1	–	–	–	1	*b	–	–	–	*b	–	–	–	
2006—238	08:40	3.400	21.01	–	–	2	–	–	–	–	1	–	–	–	1	–	–	–	–	*b	–	–	–	*b	–	–	–	
2006—271	16:30	3.211	33.32	–	–	1	–	–	–	1	2	–	–	–	1	–	–	–	1	*b	–	–	–	*b	–	–	–	
2007—069	07:54	2.163	162.6	–	–	–	–	–	–	–	–	–	–	–	–	–	–	–	–	–	–	–	–	–	–	–	–	
2007—092	18:15	2.004	23.43	–	1	–	–	–	1	2	2	–	–	1	1	–	–	–	–	*b	–	–	1	*b	–	–	–	
2007—121	04:07	1.818	28.41	–	–	–	–	–	–	–	–	–	–	–	–	–	–	–	–	–	–	–	–	–	–	–	–	
2007—152	04:50	1.634	31.02	–	1	6	–	–	1	–	1	–	–	1	–	–	–	–	–	*b	–	–	–	*b	–	–	–	
2007—182	21:34	1.489	30.69	–	13	10	4	–	–	–	1	–	–	–	2	–	–	–	1	*b	–	–	–	*b	–	–	–	
2007—200	08:56	1.433	17.47	2	12	6	1	–	–	8	5	–	–	–	1	–	–	–	1	*b	–	–	–	*b	–	–	–	
2007—222	17:12	1.396	22.34	2	25	17	3	–	1	3	2	–	–	3	–	–	–	1	3	*b	–	–	–	*b	–	–	–	
2007—243	23:21	1.402	21.25	3	25	8	1	–	3	9	2	–	–	3	5	–	–	–	1	2	*b	–	2	1	*b	–	1	–
2007—266	13:56	1.452	22.60	–	5	13	4	–	2	6	–	–	–	4	5	–	–	–	2	*b	–	–	–	*b	–	–	–	
2007—288	22:33	1.538	22.35	–	8	9	–	–	1	1	–	–	–	1	2	–	–	–	1	*b	–	–	–	*b	–	–	–	
2007—309	22:37	1.644	21.00	–	1	5	–	–	–	2	–	–	–	–	2	–	–	–	2	*b	–	–	–	*b	–	–	–	
2007—334	16:30	1.790	24.74	–	3	2	–	–	–	–	–	–	–	1	–	–	–	–	–	*b	–	–	–	*b	–	–	–	
Impacts (counted)				7 <sup>a</sup>	131 <sup>a</sup>	159	31	0 <sup>a</sup>	12	88	76	0	0	17	61	0	0	4	19	*b	0	2	2	*b	0	1	0	
Impacts (complete data)				7	131	158	31	0	12	88	76	0	0	17	61	0	0	4	19	*b	0	2	2	*b	0	1	0	
All events (complete data)				6243	132	159	31	120	12	88	76	2	0	17	61	1	0	4	19	*b	0	2	2	*b	0	1	0	

Switch-on of the instrument is indicated by horizontal lines. The heliocentric distance *R*, the lengths of the time interval Δ*t* (days) from the previous table entry, and the corresponding numbers of impacts are given for the 24 accumulators. The accumulators are arranged with increasing signal amplitude ranges (AR), with four event classes for each amplitude range (CLN = 0, 1, 2, 3); e.g. AC31 means counter for AR = 1 and CLN = 3. The Δ*t* in the first line (2005—006) is the time interval counted from the last entry in Table 2 in Paper IX. The totals of counted impacts<sup>a</sup>, of impacts with complete data, and of all events (noise plus impact events) for the entire period are given as well.

<sup>a</sup> Entries for AC01, AC11 and AC02 are the number of impacts with complete data. Due to the noise contamination of these three categories the number of impacts cannot be determined from the accumulators. The method to separate dust impacts from noise events in these three categories has been given by Baguhl et al. (1993).

<sup>b</sup> No entries are given for AC05 and AC06 because they count the overflows of accumulators AC21 and AC31 since the reprogramming in December 2004 (Paper IX).

given in the last columns. For VEF > 6, both velocity and mass values should be discarded. This occurs for 72 impacts. No intrinsic dust charge values are given (see Svestka et al., 1996, for a detailed analysis). Reliable charge measurements for interplanetary dust particles and grains in Saturn's E ring were reported for the Cassini dust detector (Kempf et al., 2004, 2006). These measurements may lead to an improved understanding of the charge measurements of Ulysses and Galileo in the future.

#### 4. Analysis

The most important impact parameter determined by the dust instrument is the positive charge measured on the ion collector, *Q<sub>i</sub>*, because it is relatively insensitive to noise. Fig. 4 shows the distribution of *Q<sub>i</sub>* for all dust particles detected from 2005 to 2007.

Ion impact charges have been detected over the entire range of six orders of magnitude in impact charge that the dust instrument can measure. One impact is close to the saturation limit of ~10<sup>-8</sup> C and may thus constitute a lower limit of the actual impact charge. The impact charge distribution of the big particles (*Q<sub>i</sub>* > 10<sup>-13</sup> C) follows a power law distribution with index -0.45 and is shown as a dashed line. This value is—within the measurement uncertainty—in agreement with earlier Ulysses measurements of 2000–2004 (-0.40; cf. Paper IX).

In the earlier 1993–2004 data set (Papers V, VII and IX) the impact charge distribution was reminiscent of three individual populations: small particles with impact charges *Q<sub>i</sub>* < 10<sup>-13</sup> C (AR1), intermediate size particles with 10<sup>-13</sup> C ≤ *Q<sub>i</sub>* ≤ 10<sup>-11</sup> C (AR2 and AR3) and the largest particles with *Q<sub>i</sub>* > 10<sup>-11</sup> C (AR4 to AR6). This is also visible in the present data set, although less pronounced. We suggest that the intermediate particles are

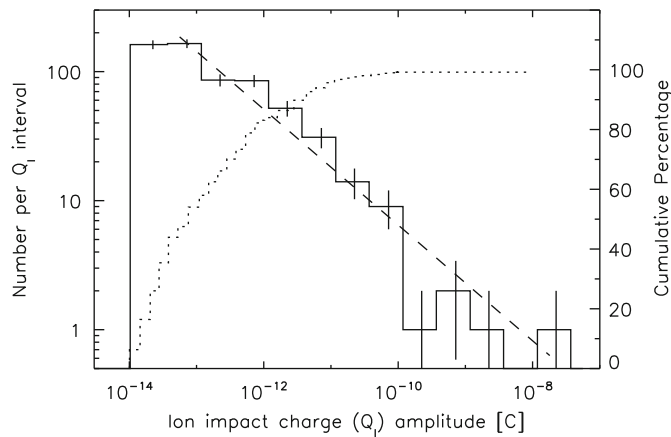


**Fig. 4.** Distribution of the impact charge amplitude  $Q_i$  for all dust particles detected from 2005 to 2007. The solid line indicates the number of impacts per charge interval, and the dotted line shows the cumulative percentage. Vertical bars indicate the  $\sqrt{n}$  statistical fluctuation. A power law fit to the data with  $Q_i > 3 \times 10^{-14}$  C is shown as a dashed line (number  $N \sim Q_i^{-0.45}$ ).

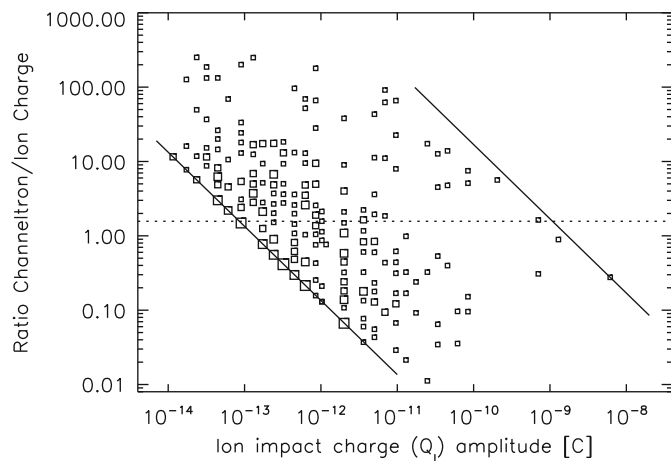


**Fig. 5.** Channeltron amplification factor  $A = Q_c/Q_i$  as a function of impact charge  $Q_i$  for all dust impacts detected between 2005 and 2007 with channeltron voltage set to  $HV = 4$ . The solid lines denote the sensitivity threshold (lower left) and the saturation limit (upper right) of the channeltron. Squares indicate dust particle impacts. The area of each square is proportional to the number of events included (the scaling of the squares is not the same as in earlier papers). The dotted horizontal line shows the mean value of the channeltron amplification  $A = 1.57$  for ion impact charges  $10^{-12}$  C  $< Q_i < 10^{-11}$  C (82 particles).

mostly of interstellar origin and the big particles are attributed to interplanetary grains (Grün et al., 1997, see also Section 5). The small particle impacts (AR1) detected over the polar regions of the Sun are candidates for being interplanetary  $\beta$ -meteoroids (Hamilton et al., 1996; Wehry and Mann, 1999; Wehry et al., 2004).

It should be noted that the charge distribution shown in Fig. 4 is very similar to the one measured with Galileo in interplanetary space between 1993 and 1995 (i.e. between 1 and 5 AU; Paper IV). In particular, the power law index of  $-0.43$  was practically identical. This indicates that both dust instruments basically detected the same dust populations in interplanetary space and that their responses to dust impacts are very similar. The only significant difference is a dip in the Ulysses charge distribution at  $2 \times 10^{-10}$  C (Fig. 4) which is also evident in all earlier Ulysses data (Papers III, V, VII and IX). In particular, it is visible in both the ecliptic and out-of-ecliptic phases of Ulysses which indicates that

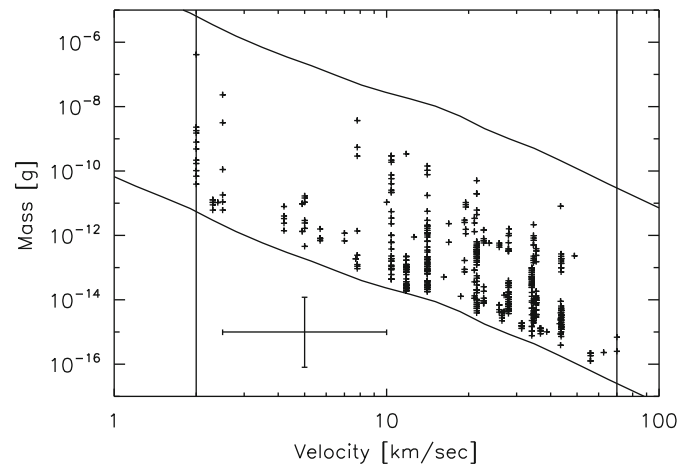


**Fig. 6.** Masses and impact velocities of all impacts recorded with the Ulysses sensor from 2005 to 2007. The lower and upper solid lines indicate the threshold and the saturation limit of the detector, respectively, and the vertical lines indicate the calibrated velocity range. A sample error bar is shown that indicates a factor of 2 uncertainty for the velocity and a factor of 10 for the mass determination.

it is not sensitive to the impact speed or the dust population of the grains. A small but much weaker dip is also seen in some but not all Galileo data sets. We therefore conclude that the dip is most likely due to an artefact in the Ulysses instrument electronics in AR5.

The ratio of the channeltron charge  $Q_c$  and the ion collector charge  $Q_i$  is a measure of the channeltron amplification  $A$ , which in turn is an important parameter for dust impact identification (Paper I). In Fig. 5 we show the charge ratio  $Q_c/Q_i$  as a function of  $Q_i$  for the 2005–2007 dust impacts with the channeltron high voltage set to 1250 V ( $HV = 4$ ). This diagram is directly comparable with similar diagrams in the previous Papers III, V and VII for  $HV = 3$  and Paper IX for  $HV = 4$ , respectively.

The mean amplification determined from particles with  $10^{-12}$  C  $\leq Q_i \leq 10^{-11}$  C and  $HV = 4$  in the 2005–2007 interval is  $A \approx 1.57$ . This value is somewhat lower than the values derived from the first five years of the mission (1990–1995; Papers III and V) and comparable to the more recent determinations (1996–2004; Papers VII and IX). It indicates that a sufficiently high channeltron amplification and stable instrument operation could be maintained with this higher voltage ( $HV = 4$ ) since 2000. It shows in particular that the channeltron degradation could be mostly counterbalanced by increasing the high voltage by one digital step. Much more severe electronics degradation was found for the Galileo dust detector during Galileo's orbital tour in the Jovian system. It was likely related to the harsh radiation environment in the magnetosphere of the giant planet (Krüger et al., 2005).

In Fig. 6 we show the masses and speeds of all dust particles detected between 2005 and 2007. As in the earlier periods before 2005, speeds occur over the entire calibrated range from 2 to 70 km s $^{-1}$ . The masses vary over almost nine orders of magnitude from  $\sim 10^{-7}$  to  $10^{-16}$  g. The mean errors are a factor of 2 for the speed and a factor of 10 for the mass. The clustering of the speed values is due to discrete steps in the rise time measurement but this quantisation is much smaller than the speed uncertainty. For many particles in the lowest two amplitude ranges (AR1 and AR2) the speed had to be computed from the ion charge signal alone which leads to the vertical striping in the lower mass range in Fig. 6 (most prominent above 10 km s $^{-1}$ ). In the higher amplitude ranges the speed could normally be calculated from both the target and the ion charge signal, resulting in a more continuous distribution in the mass–speed plane. Impact speeds below about



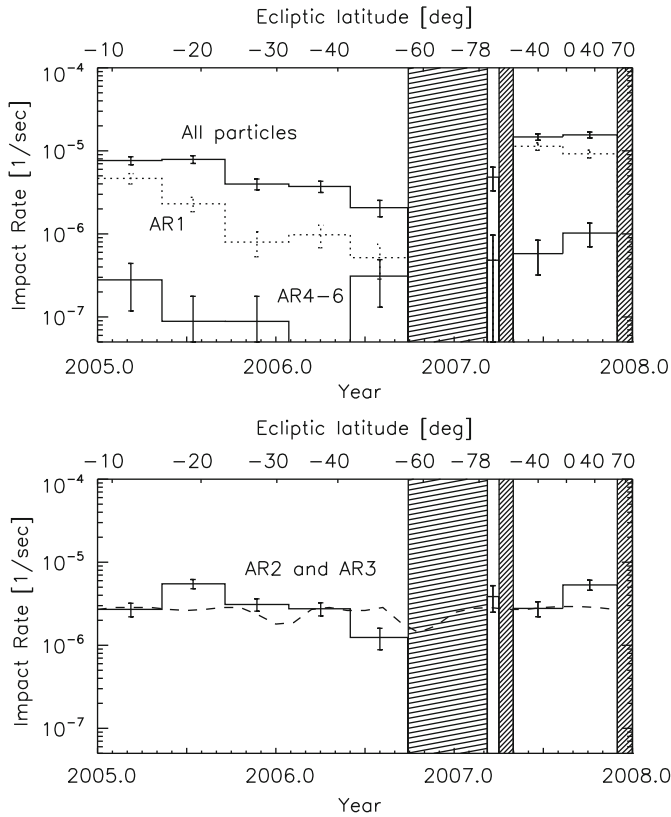


**Fig. 7.** Impact rate of dust particles detected with the Ulysses dust sensor as a function of time. The ecliptic latitude of the spacecraft is indicated at the top. Shaded areas indicate periods when the dust instrument was switched off. Upper panel: Total impact rate (upper solid histogram), impact rate of small particles (AR1, dotted histogram), and impact rate of big particles (AR4–AR6, lower solid histogram). Note that a rate of about  $10^{-7}$  impacts per second is caused by a single dust impact in the averaging interval of about 130 days. An averaging interval of only 24 days had to be used for March 2007 because the instrument was switched off before and after this period. Lower panel: impact rate of intermediate size particles (AR2 and AR3, solid histogram). A model for the rate of interstellar particles assuming a constant flux was fit to the data and is superimposed as a dashed line. Vertical bars indicate the  $\sqrt{n}$  statistical fluctuation.

$3 \text{ km s}^{-1}$  should be treated with caution because anomalous impacts onto the sensor grids or structures other than the target generally lead to prolonged rise times and hence to unnaturally low impact speeds.

### 5. Discussion

In Fig. 7 we show the dust impact rate detected in various amplitude ranges together with the total impact rate summed over all amplitude ranges. The highest overall impact rate was recorded in 2007 when Ulysses was in the inner solar system and relatively close to the ecliptic plane. It coincides with a peak in the rate of the largest particles in the three highest ion amplitude ranges (AR4–AR6). These impacts are attributed to interplanetary particles on low inclination orbits (Grün et al., 1997). The majority of them are the impacts with  $Q_i > 10^{-10} \text{ C}$  shown in Fig. 4. The impact rate of intermediate sized particles in AR2 and AR3 showed relatively little variation. This size range is dominated by interstellar impactors. The details of the various dust populations and how they are identified in the data set are discussed further below.

Fig. 8 shows the sensor orientation at the time of a particle impact (rotation angle). The largest particles (diamonds, impact charge  $Q_i \geq 8 \times 10^{-14} \text{ C}$  which roughly corresponds to AR2–6) are

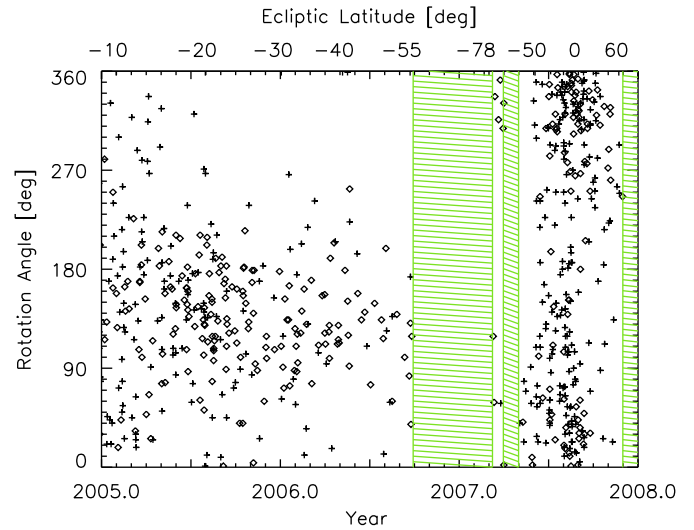


**Fig. 8.** Rotation angle vs. time for all particles detected in the 2005–2007 interval. Plus signs indicate particles with impact charge  $Q_i < 10^{-13} \text{ C}$  (AR1), diamonds those with  $Q_i > 8 \times 10^{-14} \text{ C}$  (AR2 to AR6). Ulysses’ ecliptic latitude is indicated at the top.

concentrated towards the upstream direction of interstellar helium (cf. Fig. 10, bottom panel; Witte et al., 1996; Witte, 2004; Witte et al., 2004). They have been detected with a relatively constant rate during the entire three-year period (Fig. 7). The particles with the highest ion amplitude ranges (AR4 to AR6) are not distinguished in this diagram because they cannot be separated from interstellar particles by directional arguments alone. They have to be distinguished by other means (e.g. mass and speed). In addition, their total number is so small that they constitute only a small “contamination” of the interstellar particles in Fig. 8. In the ecliptic plane at 1.3 AU, however, interplanetary particle flux dominates over interstellar flux by a factor of about 3 (in number).

#### 5.1. Interstellar dust

Interstellar particles move on hyperbolic trajectories through the solar system and approach Ulysses from the same direction as the interstellar gas. They can therefore be identified by their impact direction and their impact speed. For more details concerning the identification of interstellar impactors in the Ulysses dust data set the reader is referred to earlier investigations (Grün et al., 1994; Baguhl et al., 1995a; Frisch et al., 1999). In the Ulysses and Galileo dust data sets the interstellar impactors are mostly found in amplitude ranges AR2 and AR3.

In the earlier mission from 1993 to 2004 the impact rate of interstellar grains (as derived from the AR2 and AR3 accumulators) varied by about a factor of 2.5: between 1993 and 1995 the rate was  $\sim 2 \times 10^{-6} \text{ s}^{-1}$  (Paper V) while in the 1996–1999 interval it dropped to  $\sim 8 \times 10^{-7} \text{ s}^{-1}$  (Paper VII) and from 2000 to 2004 the average impact rate was again  $\sim 2 \times 10^{-6} \text{ s}^{-1}$  (Paper IX). In 2005/2006 the average impact rate of interstellar impactors was somewhat higher:  $\sim 3 \times 10^{-6} \text{ s}^{-1}$  (bottom panel of Fig. 7). In 2007, when Ulysses was in the inner solar system again, the impact rate derived from AR2 and AR3 was still higher. Here, however, the impact rate is not due to interstellar particles alone because of a strong contribution from interplanetary impactors.

The dashed curve in Fig. 7 (bottom panel) shows the expected impact rate of interstellar particles assuming that they approach from the direction of interstellar helium and that they move through the solar system on straight trajectories with the relative velocity of the Sun’s motion with respect to the Local Interstellar

Cloud ( $\sim 26 \text{ km s}^{-1}$ ). This assumption means dynamically that radiation pressure cancels gravity for these particles ( $\beta = 1$ ) and that their Larmor radii are large compared with the dimension of the solar system. Both assumptions are reasonable for particles with masses between  $10^{-13}$  and  $10^{-12}$  g which is the dominant size range measured for interstellar grains (Grün et al., 1997). The variation predicted by the model is caused by changes in the instrument's viewing direction with respect to the approach direction of the particles and changes in the relative velocity between the spacecraft and the particles. The dust particle flux is independent of heliocentric distance in this simple model, which gives relatively good agreement with the observed impact rate.

Ulysses has monitored the interstellar dust flow through the solar system for more than 15 years. This time period covers more than two and a half revolutions of the spacecraft about the Sun through more than  $\frac{2}{3}$  of a complete 22-year solar cycle. Thus, Ulysses measured interstellar dust during solar minimum and solar maximum conditions of the interplanetary magnetic field (IMF). The interstellar dust flux modulation due to grain interaction with the magnetic field during solar minimum could be well explained (Landgraf, 1998, 2000; Landgraf et al., 2003). By taking into account the sensor side wall in the instrument field of view we could recently improve the flux determination (Altobelli et al., 2004).

Ulysses provides a unique opportunity to compare repeated dust measurements at the same locations in the solar system for different phases of the solar cycle and the interplanetary magnetic field. In Fig. 9 we show the approach direction of interstellar grains for three selected periods when Ulysses was between approximately  $-8^\circ$  and  $-56^\circ$  ecliptic latitude during approach to the inner solar system. During these three intervals the dust detection geometry as indicated by the contour lines was very similar so that we can compare them directly. At least three differences are obvious between the three panels:

- The approach direction of the majority of grains was compatible with the flow direction of the interstellar helium gas as measured with Ulysses during all three time intervals.
- The dust flux varied by a factor of about two during the three intervals, the lowest flux being measured in the period 1999 to 2000, while the highest flux occurred in 2005/2006 (Krüger et al., 2007).
- A subset of the grains detected in 2005 shows a shift in the detected impact direction away from the ecliptic plane towards southern ecliptic latitudes (impacts in the approximate rotation angle range from  $100^\circ$  to  $240^\circ$  in the bottom panel of Fig. 9).

Our preliminary analysis indicates that this shift is about  $30^\circ$  away from the ecliptic plane towards southern ecliptic latitudes (Krüger et al., 2007). The reason for this shift remains mysterious. Whether it is connected to a secondary stream of interstellar neutral atoms shifted from the main neutral gas flow (Collier et al., 2004; Wurz et al., 2004; Nakagawa et al., 2006) is presently unclear. Given, however, that the neutral gas stream is shifted along the ecliptic plane while the shift in the dust flow is offset from the ecliptic, a connection between both phenomena seems unlikely.

Even though Ulysses' position in the heliosphere and the dust detection conditions were very similar during all three time intervals considered in Fig. 9, the configurations of the solar wind driven interplanetary magnetic field (IMF), which strongly affects the dynamics of the smallest grains, were completely different. We have to consider that the interstellar grains need approximately twenty years to travel from the heliospheric boundary to

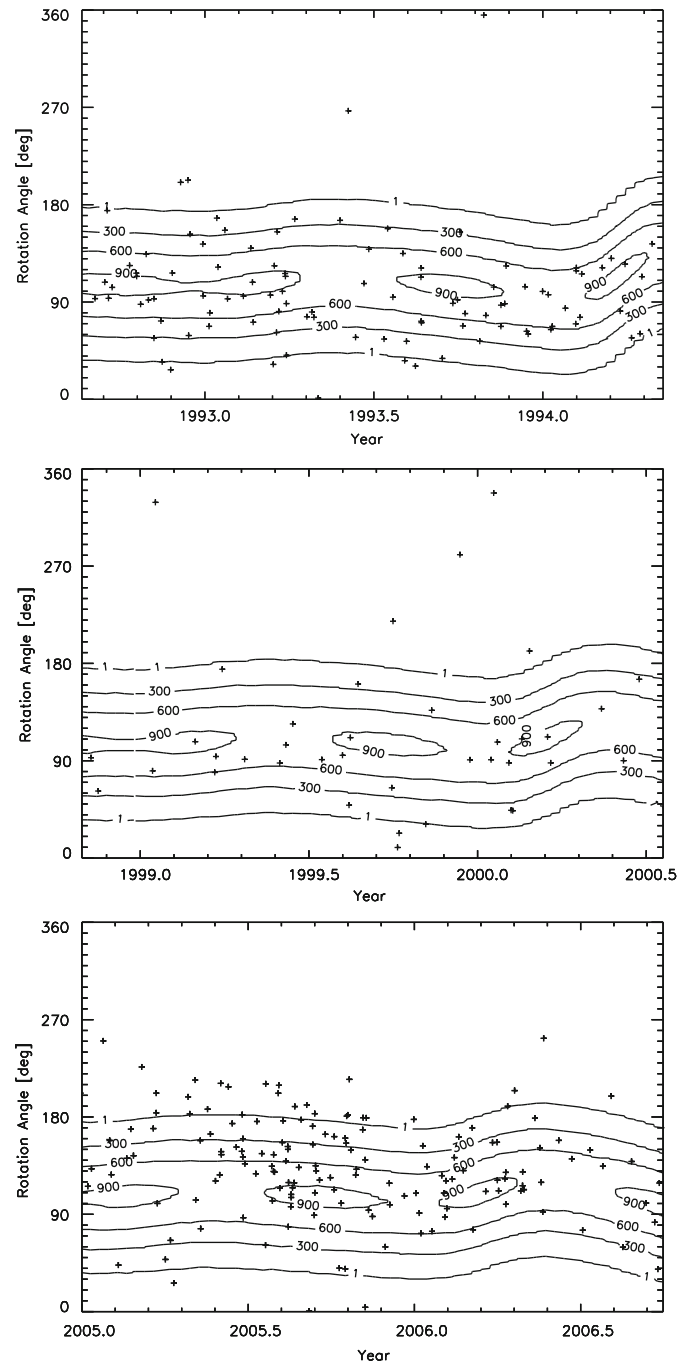


**Fig. 9.** Rotation angle vs. time for dust impacts detected during three time intervals when Ulysses was traversing the same portion of its trajectory between  $-8.5^\circ$  and  $-56^\circ$  ecliptic latitude. Contour lines show the effective sensor area for dust particles approaching from the upstream direction of interstellar helium (Witte, 2004; Witte et al., 2004). Here we show particles with impact charges  $1.5 \times 10^{-13} \text{ C} < Q_i < 10^{-11} \text{ C}$  which approximately coincides with AR2–3.

the inner solar system where they are detected by Ulysses. Thus, the effect of the IMF on the grain dynamics is the accumulated effect caused by the interaction with the IMF over several years: In the earlier time intervals (1993/1994 and 1999/2000) the grains had a recent dynamic history dominated by solar minimum conditions (Landgraf, 2000), while the grains detected during the third interval (2005/2006) had a recent history dominated by the much more disturbed solar maximum conditions of the IMF. During the solar maximum conditions the overall magnetic dipole field changed polarity. Morfill and Grün (1979) predicted that due

to this effect in a 22-year cycle, small interstellar grains experience either focussing or defocussing conditions. During these times they are systematically deflected by the solar wind magnetic field either towards or away from the solar magnetic equator plane (close to the ecliptic plane). This latter configuration likely has a strong influence on the dust dynamics and the total interstellar flux in the inner heliosphere but it has not been modelled in detail. An explanation of the grain interaction with the IMF at the recent solar maximum conditions is still pending.

Detailed modelling of the dynamics of the electrically charged dust grains in the heliosphere can give us information about the local interstellar environment of the solar system where the particles originate. The models developed by Landgraf et al. (2003) fit the observed flux variation by assuming a constant dust concentration in the local interstellar environment of our solar system. It implies that the local interstellar dust phase must be homogeneously distributed over length scales of 50 AU, which is the distance travelled by the Sun during the measurement period of Ulysses from 1992 to 2002. This conclusion is supported by the more recent Ulysses data until the end of 2004 (Paper IX). Our latest Ulysses dust data of 2005/2006, on the other hand, put a question mark onto this conclusion because if the observed shift in impact direction turns out to be intrinsic, it would imply that this homogeneity breaks down on larger length scales.

## 5.2. Interplanetary dust

Fig. 10 shows the data (AR3 to AR6) from launch in 1990 until the end of the Ulysses mission in 2007 and compares them with two meteoroid environment models by Divine (1993) and Staubach et al. (1997). For most of the mission time, excluding the ecliptic plane crossings in 1995, 2001 and 2007 the Divine model predicts impacts from a very broad range of directions, with spin angles from  $45^\circ$  to  $300^\circ$ . The impactors belong mostly to the so-called “halo” population which was introduced in the model to explain the Pioneer data (Divine, 1993). The Ulysses directionality of the impacts had not been available at the time of construction of the model, and the data do not fit well with a “halo” population. In contrast, the Staubach et al. (1997) model

was compared with 5 years of Ulysses data from the craft’s first orbit about the Sun, taking the crucial directional information into account. It is in better agreement with the data and has been confirmed by Ulysses’ second and third orbits. It places most of the impacts into the spin angle range from  $30^\circ$  to  $120^\circ$ . These are due to interstellar dust flowing through the solar system (Grün et al., 1994).

One more observation from these plots is that both the Divine and Staubach models predict higher flux during the ecliptic plane crossings than the data permit. The time dependence of the interstellar dust flux was asserted after the meteoroid models under review had been constructed (Landgraf, 2000). However, the disagreement at the ecliptic plane crossings was not anticipated, since almost all data incorporated in the models were taken from the ecliptic plane. Possible explanations of the discrepancy are the roughness of model fits as well as different representations of the data taken for model adjustments and displayed in Fig. 10. While Fig. 10 selects all impacts above a fixed threshold of charge released, the models were fitted using more uncertain inferred mass thresholds. The inference of mass is based on speed determination that is uncertain by a factor of 2.

## 5.3. $\beta$ -meteoroids

When Ulysses was in the inner solar system in 1995 and in 2001, maxima were evident in the impact rate of the smallest particles (AR1; Papers V and IX). A similar maximum in the inner solar system occurred again in 2007 (Fig. 7; top panel). Although in all three cases the maximum was reached during a short period around ecliptic plane crossing, many particles were also detected at high ecliptic latitudes. These grains are attributed to a population of submicron-sized interplanetary particles whose dynamics is dominated by solar radiation pressure. They move on escape trajectories from the solar system ( $\beta$ -meteoroids, Baguhl et al., 1995b; Hamilton et al., 1996).  $\beta$ -meteoroids were identified with Ulysses over the Sun’s poles in 1994/1995 (Wehry and Mann, 1999) and 2000/2001 (Wehry et al., 2004). Due to the detection geometry, however, they were undetectable outside these periods, explaining the lower impact rates in AR1.  $\beta$ -meteoroids were detectable again from mid-2006 until early-2008 (Wehry et al., 2004). An independent potential detection of  $\beta$ -meteoroids

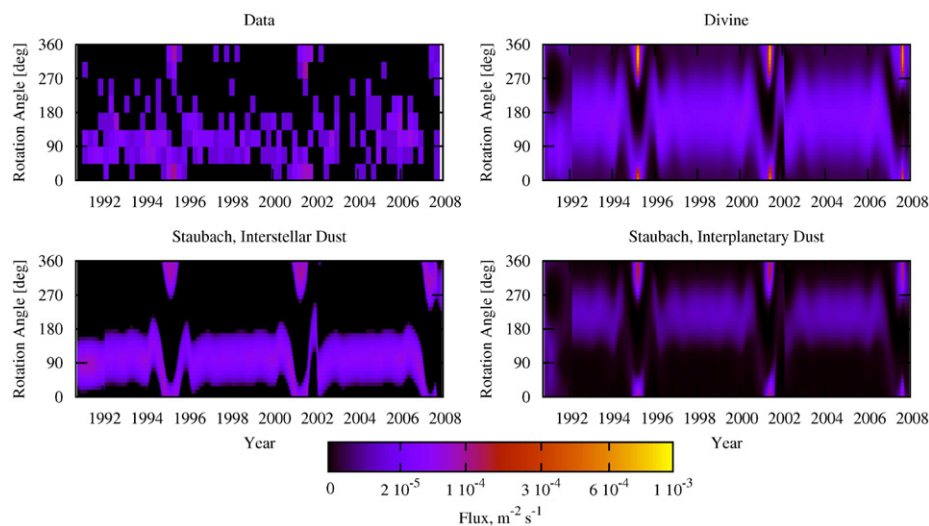


**Fig. 10.** Particle fluxes onto the Ulysses dust detector as seen in the data (AR3 to AR6, top left panel) and predicted by the meteoroid environment models by Divine (1993, top right panel) and Staubach et al. (1997, two bottom panels). The Jupiter encounter in 1992 is best seen on the model plots as a sharp swing in directionality of impacts caused by the rotation of spacecraft velocity relative to the giant planet. The ecliptic plane crossings near the perihelia in 1995, 2001 and 2007 are marked by the high impact rates due to the number density of dust increase near the Sun and high speed of Ulysses relative to this dust. As the spacecraft moved north at the times of the crossings, the meteoroids came from the ecliptic north as well (rotation angle 0).

was recently reported from the plasma wave instrument on board the STEREO spacecraft (Meyer-Vernet et al., 2009).

Wehry and Mann (1999) and Wehry et al. (2004) identified a significant asymmetry in the flux of these particles between the northern and the southern hemisphere from the first two heliocentric orbits of Ulysses, the reason of which is presently unknown. A comprehensive analysis of these three data sets will be the subject of a future investigation and may reveal whether the asymmetry is connected with (for example) the solar cycle variation of the interplanetary magnetic field.

## 6. Conclusions

In this paper, the eleventh and final in a series of Ulysses and Galileo dust data papers, we present data from the Ulysses dust instrument for the period January 2005 to November 2007. In this time interval, starting from a heliocentric distance of 5.3 AU close to aphelion, the spacecraft approached the Sun, passed over the Sun's south pole, crossed the ecliptic plane at 1.4 AU heliocentric distance and reached a northern ecliptic latitude of 60°.

A total number of 609 dust impacts were recorded during this period. Together with 6110 impacts recorded in interplanetary space and near Jupiter between Ulysses' launch in October 1990 and December 2004 (Grün et al., 1995a; Krüger et al., 1999b, 2001b, 2006a), the complete dust data set measured during the entire Ulysses mission consists of 6719 impacts. Given its temporal coverage and Ulysses' unique orbital orientation, the Ulysses dust data set will be a treasure for decades to come.

The total recorded dust impact rate dropped from an initial value of 0.7 impacts per day in 2005 when Ulysses was at low ecliptic latitudes to a value of 0.3 impacts at higher latitudes. Most of the detected impacts were due to particles of interstellar origin, in particular at higher ecliptic latitudes, a minor fraction being interplanetary particles. A maximum of 1.5 per day was measured in 2007 in the inner solar system; here the majority of the grains were of interplanetary origin.

The measurements from the entire Ulysses mission since launch in 1990 are in disagreement with the interplanetary dust flux model by Divine (1993). Instead, they are well matched by the model of Staubach et al. (1997) which was originally developed with a shorter data set from the first Ulysses orbit and with the dust measurements from Galileo's interplanetary cruise.

Noise tests performed regularly during the three years period revealed no degradation in the noise sensitivity of the dust instrument, and the nominal instrument operational configuration remained unchanged during the entire period. In particular, no change in the channeltron high voltage setting was required.

With Ulysses we had the unprecedented opportunity to measure dust in interplanetary space for approximately 17 years. In particular, due to the unique orientation of Ulysses' orbital plane approximately perpendicular to the flow direction of the interstellar dust through the solar system and the spacecraft's 6-year revolution period about the Sun, we obtained dust measurements from three traverses of the same spatial region at southern ecliptic latitudes. These passes were separated by six years in time and were obtained at different phases of the solar cycle. Variations in the interstellar dust flux by a factor of three are evident during the entire mission. Flux variations until 2002 have been explained by the interaction of the dust grains with the time-varying interplanetary magnetic field, while detailed modelling of the later data is still pending. The data obtained in 2005/

2006 reveal an approximately 30° shift in the approach direction of the grains away from the approach direction of the interstellar helium gas. The reason for this shift remains mysterious and will be the subject of a future investigation.

Even though this is the final paper in our series of Ulysses dust data papers published during the last 15 years, the evaluation of this unique data set is continuing. A list of specific open questions raised in this and earlier data papers includes:

- *β-meteoroids*: The detailed evaluation of the measurements from Ulysses' third solar orbit is still pending. Open questions include the north-south asymmetry in the measured flux and the heliocentric distance range where these grains are generated. More measurements from other spacecraft (e.g. STEREO) would be advantageous to answer these questions.
- *Comparison with Pioneer 10 and 11 measurements*: The flux of particles with  $m \geq 10^{-9}$  g as measured with Ulysses is about a factor of five lower than expected from the Pioneer 10 and 11 measurements. Potential reasons for this discrepancy are errors in the mass calibrations of the Ulysses and/or Pioneer detectors in this mass range, many of the Pioneer detections may not be due to actual meteoroid impacts, or the dust grains detected by Pioneer belong to a population of dust which could not or only partially be detected with Ulysses (Krüger et al., 1999b). Measurements with New Horizons in the outer solar system may shed new light onto this question.
- *Interstellar dust*: Earlier comprehensive investigations of the interstellar impactors were mostly performed in the late 1990s and relied upon the significantly smaller data set available at the time. In the meantime, until the end of the Ulysses mission, the interstellar dust data set has grown by at least a factor of two so that a complete re-analysis of the entire data set is worthwhile and can give new insights into, e.g., the grain dynamics inside the heliosphere and into the conditions in the local interstellar environment where these grains originate. In particular, the reason for the observed 30° shift remains an open question.
- *Interplanetary dust*: The interplanetary dust model by Divine (1993) was developed before the Ulysses data became available and the model by Staubach et al. (1997) used only data from within the ecliptic plane and from a fraction of Ulysses' first heliocentric orbit. A new model is presently being developed by Dikarev et al. (2005) which will incorporate infrared observations of the zodiacal cloud by the COBE DIRBE instrument, in situ flux measurements by the dust detectors on board Galileo and Ulysses, and the crater size distributions on lunar rock samples retrieved by the Apollo missions.

## Acknowledgements

We dedicate this work to the memory of Dietmar Linkert who passed away in spring 2009. He was Principal Engineer for space instruments at MPI für Kernphysik including the dust instruments flown on the HEOS-2, Helios, Galileo, Ulysses and Cassini missions. His friends and colleagues around the world appreciated his experience and sought his professional advice. We thank the Ulysses project at ESA and NASA/JPL for effective and successful mission operations. This work has been supported by the Deutsches Zentrum für Luft- und Raumfahrt e.V. (DLR) under Grants 50 ON 9107 and 50 QJ 9503. Support by Max-Planck-Institut für Kernphysik and Max-Planck-Institut für Sonnensystemforschung is also gratefully acknowledged. The authors also



wish to thank two anonymous referees for their valuable comments for the manuscript.

## Appendix A. Supplementary data

Supplementary data associated with this article can be found in the online version, at doi: [10.1016/j.pss.2009.11.002](https://doi.org/10.1016/j.pss.2009.11.002)

## References

- Altobelli, N., Kempf, S., Krüger, H., Landgraf, M., Srama, R., Grün, E., 2005a. In-situ monitoring of interstellar dust in the inner solar system. In: AIP Conference Proceedings 761: The Spectral Energy Distributions of Gas-Rich Galaxies, pp. 149–152.
- Altobelli, N., Kempf, S., Krüger, H., Landgraf, M., Roy, M., Grün, E., 2005b. Interstellar dust flux measurements by the Galileo dust instrument between Venus and Mars orbit. *Journal of Geophysical Research* 110, 7102–7115.
- Altobelli, N., Kempf, S., Landgraf, M., Srama, R., Dikarev, V., Krüger, H., Moragas-Klostermeyer, G., Grün, E., 2003. Cassini between Venus and Earth: detection of interstellar dust. *Journal of Geophysical Research* 108 (A10), 1–7.
- Altobelli, N., Moissl, R., Krüger, H., Landgraf, M., Grün, E., 2004. Influence of wall impacts on the Ulysses dust detector in modelling the interstellar dust flux. *Planetary and Space Science* 52, 1287–1295.
- Baggaley, W.J., Neslušan, L., 2002. A model of the heliocentric orbits of a stream of Earth-impacting interstellar meteoroids. *Astronomy and Astrophysics* 382, 1118–1124.
- Baguhl, M., Grün, E., Linkert, G., Linkert, D., Siddique, N., 1993. *Planetary and Space Science* 41, 1085.
- Baguhl, M., Grün, E., Hamilton, D.P., Linkert, G., Riemann, R., Staubach, P., 1995a. The flux of interstellar dust observed by Ulysses and Galileo. *Space Science Reviews* 72, 471–476.
- Baguhl, M., Hamilton, D.P., Grün, E., Dermott, S.F., Fechtig, H., Hanner, M.S., Kissel, J., Lindblad, B.A., Linkert, D., Linkert, G., Mann, I., McDonnell, J.A.M., Morfill, G.E., Polanskey, C., Riemann, R., Schwehm, G.H., Staubach, P., Zook, H.A., 1995b. Dust measurements at high ecliptic latitudes. *Science* 268, 1016–1020.
- Balogh, A., Marsden, R., Smith, E.E., 2001. *The Heliosphere Near Solar Minimum: The Ulysses Perspective*. Springer Praxis, Springer, Berlin, Heidelberg, New York.
- Collier, M.R., Moore, T.E., Simpson, D., Roberts, A., Szabo, A., Fuselier, S., Wurz, P., Lee, M.A., Tsurutani, B.T., 2004. An unexplained 10–40° shift in the location of some diverse neutral atom data at 1 AU. *Advances in Space Research* 34, 166–171.
- Czechowski, A., Mann, I., 2003a. Local interstellar cloud grains outside the heliopause. *Astronomy and Astrophysics* 410, 165–173.
- Czechowski, A., Mann, I., 2003b. Penetration of interstellar grains into the Heliosphere. *Journal of Geophysical Research* 108 (A10), 8038. [10.1029/2003JA009917](https://doi.org/10.1029/2003JA009917).
- Dikarev, V., Jehn, R., Grün, E., 2002. Towards a new model of the interplanetary meteoroid environment. *Advances in Space Research* 29 (8), 1171–1175.
- Dikarev, V., Grün, E., Baggaley, J., Galligan, D., Landgraf, M., Jehn, R., 2005. The new ESA meteoroid model. *Advances in Space Research* 35, 1282–1289.
- Divine, N., 1993. Five populations of interplanetary meteoroids. *Journal of Geophysical Research* 98, 17029–17048.
- Flandes, A., Krüger, H., 2007. Solar wind modulation of Jupiter dust stream detection. In: Krüger, H., Graps, A.L. (Eds.), *Dust in Planetary Systems*, ESA SP-643, pp. 87–90.
- Frisch, P.C., Dorschner, J., Geiß, J., Greenberg, J.M., Grün, E., Landgraf, M., Hoppe, P., Jones, A.P., Krätschmer, W., Linde, T.J., Morfill, G.E., Reach, W.T., Slavin, J., Vestka, J., Witt, A., Zank, G.P., 1999. Dust in the local interstellar wind. *Astrophysical Journal* 525, 492–516.
- Frisch, P.C., Slavin, J.D., 2003. The chemical composition and gas-to-dust mass ratio of nearby interstellar matter. *Astrophysical Journal* 594, 844–858.
- Graps, A.L., Grün, E., Svedhem, H., Krüger, H., Horányi, M., Heck, A., Lammers, S., 2000. Io as a source of the Jovian dust streams. *Nature* 405, 48–50.
- Grün, E., Fechtig, H., Hanner, M.S., Kissel, J., Lindblad, B.A., Linkert, D., Maas, D., Morfill, G.E., Zook, H.A., 1992a. The Galileo dust detector. *Space Science Reviews* 60, 317–340.
- Grün, E., Fechtig, H., Kissel, J., Linkert, D., Maas, D., McDonnell, J.A.M., Morfill, G.E., Schwehm, G.H., Zook, H.A., Giese, R.H., 1992b. The Ulysses dust experiment. *Astronomy and Astrophysics, Supplement* 92, 411–423.
- Grün, E., Zook, H.A., Baguhl, M., Balogh, A., Bame, S.J., Fechtig, H., Forsyth, R., Hanner, M.S., Horányi, M., Kissel, J., Lindblad, B.A., Linkert, D., Linkert, G., Mann, I., McDonnell, J.A.M., Morfill, G.E., Phillips, J.L., Polanskey, C., Schwehm, G.H., Siddique, N., Staubach, P., Vestka, J., Taylor, A., 1993. Discovery of Jovian dust streams and interstellar grains by the Ulysses spacecraft. *Nature* 362, 428–430.
- Grün, E., Gustafson, B.E., Mann, I., Baguhl, M., Morfill, G.E., Staubach, P., Taylor, A., Zook, H.A., 1994. Interstellar dust in the heliosphere. *Astronomy and Astrophysics* 286, 915–924.
- Grün, E., Baguhl, M., Divine, N., Fechtig, H., Hamilton, D.P., Hanner, M.S., Kissel, J., Lindblad, B.A., Linkert, D., Linkert, G., Mann, I., McDonnell, J.A.M., Morfill, G.E., Polanskey, H.A., Riemann, R., Schwehm, G.H., Siddique, N., Staubach, P., Zook, H.A., 1995a. Two years of Ulysses dust data. *Planetary and Space Science* 43, 971–999 (Paper III).
- Grün, E., Baguhl, M., Divine, N., Fechtig, H., Hamilton, D.P., Hanner, M.S., Kissel, J., Lindblad, B.A., Linkert, D., Linkert, G., Mann, I., McDonnell, J.A.M., Morfill, G.E., Polanskey, C., Riemann, R., Schwehm, G.H., Siddique, N., Staubach, P., Zook, H.A., 1995b. Three years of Galileo dust data. *Planetary and Space Science* 43, 953–969 (Paper II).
- Grün, E., Baguhl, M., Hamilton, D.P., Kissel, J., Linkert, D., Linkert, G., Riemann, R., 1995c. Reduction of Galileo and Ulysses dust data. *Planetary and Space Science* 43, 941–951 (Paper I).
- Grün, E., Staubach, P., Baguhl, M., Hamilton, D.P., Zook, H.A., Dermott, S.F., Gustafson, B.A., Fechtig, H., Kissel, J., Linkert, D., Linkert, G., Srama, R., Hanner, M.S., Polanskey, C., Horányi, M., Lindblad, B.A., Mann, I., McDonnell, J.A.M., Morfill, G.E., Schwehm, G.H., 1997. South–North and radial traverses through the interplanetary dust cloud. *Icarus* 129, 270–288.
- Grün, E., Krüger, H., Graps, A., Hamilton, D.P., Heck, A., Linkert, G., Zook, H., Dermott, S.F., Fechtig, H., Gustafson, B., Hanner, M., Horányi, M., Kissel, J., Lindblad, B., Linkert, G., Mann, I., McDonnell, J.A.M., Morfill, G.E., Polanskey, C., Schwehm, G.H., Srama, R., 1998. Galileo observes electromagnetically coupled dust in the Jovian magnetosphere. *Journal of Geophysical Research* 103, 20011–20022.
- Grün, E., Landgraf, M., 2000. Collisional consequences of big interstellar grains. *Journal of Geophysical Research* 105 (A5), 10291–10298.
- Grün, E., Krüger, H., Landgraf, M., 2001. Cosmic dust. In: Balogh, A., Marsden, R., Smith, E. (Eds.), *The Heliosphere at Solar Minimum: The Ulysses Perspective*. Springer Praxis, Berlin, pp. 373–404.
- Hamilton, D.P., Burns, J.A., 1993. Ejection of dust from Jupiter's gossamer ring. *Nature* 364, 695–699.
- Hamilton, D.P., Grün, E., Baguhl, M., 1996. Electromagnetic escape of dust from the solar system. In: Gustafson, B.A.S., Hanner, M.S. (Eds.), *Physics, Chemistry and Dynamics of Interplanetary Dust*, ASP Conference Series, vol. 104, pp. 31–34.
- Horányi, M., Morfill, G.E., Grün, E., 1993. Mechanism for the acceleration and ejection of dust grains from Jupiter's magnetosphere. *Nature* 363, 144–146.
- Horányi, M., Grün, E., Heck, A., 1997. Modeling the Galileo dust measurements at Jupiter. *Geophysical Research Letters* 24, 2175–2178.
- Jones, G.H., Balogh, A., 2003. A survey of strong interplanetary field enhancements at Ulysses. *Icarus* 166, 297–310.
- Kempf, S., Srama, R., Altobelli, N., Auer, S., Tschernjajski, V., Bradley, J., Burton, M.E., Helfert, S., Johnson, T.V., Krüger, H., Moragas-Klostermeyer, G., Grün, E., 2004. Cassini between Earth and asteroid belt: first in-situ charge measurements of interplanetary grains. *Icarus* 171, 317–335.
- Kempf, S., Beckmann, U., Srama, R., Horányi, M., Auer, S., Grün, E., 2006. The electrostatic potential of E ring particles. *Planetary and Space Science* 54, 999–1006.
- Krüger, H., Grün, E., Hamilton, D.P., Baguhl, M., Dermott, S.F., Fechtig, H., Gustafson, B.A., Hanner, M.S., Horányi, M., Kissel, J., Lindblad, B.A., Linkert, D., Linkert, G., Mann, I., McDonnell, J.A.M., Morfill, G.E., Polanskey, C., Riemann, R., Schwehm, G.H., Srama, R., Zook, H.A., 1999a. Three years of Galileo dust data: II; 1993 to 1995. *Planetary and Space Science* 47, 85–106 (Paper IV).
- Krüger, H., Grün, E., Landgraf, M., Baguhl, M., Dermott, S.F., Fechtig, H., Gustafson, B.A., Hamilton, D.P., Hanner, M.S., Horányi, M., Kissel, J., Lindblad, B., Linkert, D., Linkert, G., Mann, I., McDonnell, J.A.M., Morfill, G.E., Polanskey, C., Schwehm, G.H., Srama, R., Zook, H.A., 1999b. Three years of Ulysses dust data: 1993 to 1995. *Planetary and Space Science* 47, 363–383 (Paper V).
- Krüger, H., Grün, E., Graps, A.L., Bindschadler, D.L., Dermott, S.F., Fechtig, H., Gustafson, B.A., Hamilton, D.P., Hanner, M.S., Horányi, M., Kissel, J., Lindblad, B., Linkert, D., Linkert, G., Mann, I., McDonnell, J.A.M., Morfill, G.E., Polanskey, C., Schwehm, G.H., Srama, R., Zook, H.A., 2001a. One year of Galileo dust data from the Jovian system: 1996. *Planetary and Space Science* 49, 1285–1301 (Paper VI).
- Krüger, H., Grün, E., Landgraf, M., Dermott, S.F., Fechtig, H., Gustafson, B.A., Hamilton, D.P., Hanner, M.S., Horányi, M., Kissel, J., Lindblad, B., Linkert, D., Linkert, G., Mann, I., McDonnell, J.A.M., Morfill, G.E., Polanskey, C., Schwehm, G.H., Srama, R., Zook, H.A., 2001b. Four years of Ulysses dust data: 1996 to 1999. *Planetary and Space Science* 49, 1303–1324 (Paper VII).
- Krüger, H., Grün, E., Linkert, D., Linkert, G., Moissl, R., 2005. Galileo long-term dust monitoring in the Jovian magnetosphere. *Planetary and Space Science* 53, 1109–1120.
- Krüger, H., Altobelli, N., Anweiler, B., Dermott, S.F., Dikarev, V., Graps, A.L., Grün, E., Gustafson, B.A., Hamilton, D.P., Hanner, M.S., Horányi, M., Kissel, J., Landgraf, M., Lindblad, B., Linkert, D., Linkert, G., Mann, I., McDonnell, J.A.M., Morfill, G.E., Polanskey, C., Schwehm, G.H., Srama, R., Zook, H.A., 2006a. Five years of Ulysses dust data: 2000 to 2004. *Planetary and Space Science* 54, 932–956 (Paper IX).
- Krüger, H., Bindschadler, D., Dermott, S.F., Graps, A.L., Grün, E., Gustafson, B.A., Hamilton, D.P., Hanner, M.S., Horányi, M., Kissel, J., Lindblad, B., Linkert, D., Linkert, G., Mann, I., McDonnell, J.A.M., Moissl, R., Morfill, G.E., Polanskey, C., Schwehm, G.H., Srama, R., Zook, H.A., 2006b. Galileo dust data from the Jovian system: 1997 to 1999. *Planetary and Space Science* 54, 879–910 (Paper VIII).
- Krüger, H., Graps, A.L., Hamilton, D.P., Flandes, A., Forsyth, R.J., Horányi, M., Grün, E., 2006c. Ulysses Jovian latitude scan of high-velocity dust streams originating from the Jovian system. *Planetary and Space Science* 54, 919–931.
- Krüger, H., Landgraf, M., Altobelli, N., Grün, E., 2007. Interstellar dust in the solar system. *Space Science Reviews* 130, 401–408.

- Krüger, H., Grün, E., 2009. Interstellar dust inside and outside the heliosphere. In: Linsky, J., Izmodenov, V., Möbius, E. (Eds.), *From the Outer Heliosphere to the Local Bubble*. Springer, Heidelberg.
- Krüger, H., Bindschadler, D., Dermott, S.F., Graps, A.L., Grün, E., Gustafson, B.A., Hamilton, D.P., Hanner, M.S., Horányi, M., Kissel, J., Linkert, D., Linkert, G., Mann, I., McDonnell, J.A.M., Moissl, R., Morfill, G.E., Polansky, C., Roy, M., Schwehm, G.H., Srama, R., 2010. Galileo dust data from the Jovian system: 2000 to 2003. *Planetary and Space Science*, Paper X, under revision.
- Landgraf, M., 1998. Modellierung der dynamik und interpretation der in-situ-messung interstellaren staubs in der lokalen Umgebung des Sonnensystems. Ph.D. Thesis, Ruprecht-Karls-Universität, Heidelberg.
- Landgraf, M., Augustsson, K., Grün, E., Gustafson, B.A.S., 1999. Deflection of the local interstellar dust flow by solar radiation pressure. *Science* 286, 2319–2322.
- Landgraf, M., 2000. Modelling the motion and distribution of interstellar dust inside the heliosphere. *Journal of Geophysical Research* 105 (A5), 10303–10316.
- Landgraf, M., Baggeley, W.J., Grün, E., Krüger, H., Linkert, G., 2000. Aspects of the mass distribution of interstellar dust grains in the solar system from in situ measurements. *Journal of Geophysical Research* 105 (A5), 10343–10352.
- Landgraf, M., Krüger, H., Altabelli, N., Grün, E., 2003. Penetration of the Heliosphere by the interstellar dust stream during solar maximum. *Journal of Geophysical Research* 108, 1–5.
- Mann, I., Grün, E., Wilck, M., 1996. The contribution of Asteroid dust to the interplanetary dust cloud: the impact of ULYSSES results on the understanding of dust production in the Asteroid belt and of the formation of the IRAS dust bands. *Icarus* 120, 399–407.
- Mann, I., Kimura, H., 2000. Interstellar dust properties derived from mass density, mass distribution, and flux rates in the heliosphere. *Journal of Geophysical Research* 105 (A5), 10317–10328.
- Mann, I., Kimura, H., Biesecker, D.A., Tsurutani, B.T., Grün, E., McKibben, R.B., Liou, J.-C., MacQueen, R.M., Mukai, T., Guhathakurta, M., Lamy, P., 2004. Dust near the sun. *Space Science Reviews* 110, 269–305.
- Mann, I., Czechowski, A., 2005. Dust destruction and ion formation in the inner solar system. *Astrophysical Journal, Letters* 621, L73–L76.
- Meyer-Vernet, N., Maksimovic, M., Czechowski, A., Mann, I., Zouganelis, I., Goetz, K., Kaiser, M.L., St. Cyr, O.C., Bougeret, J.-L., Bale, S.D., 2009. Dust detection by the wave instrument on STEREO: nanoparticles picked up by the solar wind? *Solar Physics* 256, 463–474.
- Morfill, G.E., Grün, E., 1979. The motion of charged dust particles in interplanetary space II—Interstellar grains. *Planetary and Space Science* 27, 1283–1292.
- Nakagawa, H., Bzowski, M., Yamazaki, A., Fukunishi, H., Watanabe, S., Takahashi, Y., Taguchi, M., 2006. Secondary population of interstellar neutrals seems deflected to the side. In: 36th COSPAR Scientific Assembly, COSPAR, vol. 36, Plenary Meeting, p. 1170.
- Staubach, P., Grün, E., Jehn, R., 1997. The meteoroid environment near earth. *Advances in Space Research* 19, 301–308.
- Stone, R.G., Bougeret, J.L., Caldwell, J., Canu, P., de Conchy, Y., Cornilleau-Wehrin, N., Desch, M.D., Fainberg, J., Goetz, K., Goldstein, M.L., Harvey, C.C., Hoang, S., Howard, R., Kaiser, M.L., Kellogg, P., Klein, B., Knoll, R., Lecacheux, A., Langyel-Frey, D., MacDowall, R.J., Manning, R., Meetre, C.A., Meyer, A., Monge, N., Monson, S., Nicol, G., Reiner, M.J., Steinbert, J.L., Torres, E., de Villedary, C., Wouters, F., Zarka, P., 1992. The unified radio and plasma wave investigation. *Astronomy and Astrophysics, Supplement* 92, 291–316.
- Svestka, J., Auer, S., Baguhl, M., Grün, E., 1996. Measurements of dust electric charges by the Ulysses and Galileo dust detectors. In: Gustafson, B.A., Hanner, M.S. (Eds.), *Physics, Chemistry and Dynamics of Interplanetary Dust*, ASP Conference Series, vol. 104, pp. 481–484.
- Taylor, A.D., Baggeley, W.J., Steel, D.I., 1996. Discovery of interstellar dust entering the Earth's atmosphere. *Nature* 380, 323–325.
- Wehry, A., Mann, I., 1999. Identification of  $\beta$ -meteoroids from measurements of the dust detector onboard the Ulysses spacecraft. *Astronomy and Astrophysics* 341, 296–303.
- Wehry, A., Krüger, H., Grün, E., 2004. Analysis of Ulysses data: radiation pressure effects on dust particles. *Astronomy and Astrophysics* 419, 1169–1174.
- Wenzel, K., Marsden, R., Page, D., Smith, E., 1992. The Ulysses mission. *Astronomy and Astrophysics, Supplement* 92, 207–219.
- Willis, M.J., Burchell, M., Ahrens, T.J., Krüger, H., Grün, E., 2005. Decreased values of cosmic dust number density estimates in the solar system. *Icarus* 176, 440–452.
- Witte, M., Banaszkiwicz, H., Rosenbauer, H., 1996. Recent results on the parameters of interstellar helium from the Ulysses/GAS experiment. *Space Science Reviews* 78 (1/2), 289–296.
- Witte, M., 2004. Kinetic parameters of interstellar neutral helium. Review of results obtained during one solar cycle with the Ulysses/GAS-instrument. *Astronomy and Astrophysics* 426, 835–844.
- Witte, M., Banaszkiwicz, M., Rosenbauer, H., McMullin, D., 2004. Kinetic parameters of interstellar neutral helium: updated results from the Ulysses/GAS instrument. *Advances in Space Research* 34, 61–65.
- Wurz, P., Collier, M.R., Moore, T.E., Simpson, D., Fuselier, S., and Lennartson, W., 2004. Possible origin of the secondary stream of neutral fluxes at 1 AU. In: Florinski, V., Pogorelov, N.V., Zank, G.P. (Eds.), *Physics of the Outer Heliosphere*. American Institute of Physics Conference Series, vol. 719, pp. 195–200.
- Zook, H.A., Grün, E., Baguhl, M., Hamilton, D.P., Linkert, G., Linkert, D., Liou, J.-C., Forsyth, R., Phillips, J.L., 1996. Solar wind magnetic field bending of Jovian dust trajectories. *Science* 274, 1501–1503.